

1 **Cumulative and individual impacts of the human
2 footprint on similarity to high ecological integrity
3 reference states.**

4 **Evan Muise¹, Nicholas Coops¹, Txomin Hermosilla², Chris Mulverhill¹, Cole
5 Burton¹, Stephen Ban³**

6 ¹Department of Forest Resource Management, University of British Columbia, Vancouver, British
7 Columbia, Canada,

8 ²Canadian Forest Service (Pacific Forestry Centre), Natural Resources Canada, Victoria, British
9 Columbia, Canada,

10 ³BC Parks, Government of British Columbia, Victoria, British Columbia, Canada,

11 **Abstract**

12 Forests with high ecological integrity have natural or near natural ecosystem struc-
 13 ture, function, and composition, are home to large amounts of biodiversity, and
 14 provide integral ecosystem services. Anthropogenic pressures such as habitat loss,
 15 overexploitation, and land use changes are leading to the degradation or loss of
 16 high integrity forests. As a result, it is important to be able to locate and assess the
 17 quality of forests stands across wide swaths of land. Remote sensing is increasingly
 18 capable of making these assessments, through new data such as wall to wall metrics
 19 of forest structure and productivity. In this paper, we demonstrate a method to as-
 20 sess similarity to known high quality reference states using coarsened exact matching
 21 and the sigma dissimilarity metric. Using this dissimilarity metric, we can assess
 22 how far, in structural and functional space, every forest stand across Vancouver Is-
 23 land is to a comparable forest found in the oldest and largest protected area on the
 24 island, Strathcona Provincial Park. We further assess how cumulative and individ-
 25 ual anthropogenic pressures are influencing ecological dissimilarity. We found that
 26 cumulative anthropogenic pressures influence the vertical layering of forests (canopy
 27 height and structural complexity), but do not influence forest energy availability or
 28 energy seasonality. Further, individual anthropogenic pressures increase dissimilar-
 29 ity for the majority of forest structural attributes, and population density reduces
 30 similarity to highly seasonal forests. Our results demonstrate that applying strict
 31 matching procedures and the sigma dissimilarity metric can be used to assess ecosys-
 32 tem similarity, which could be useful when examining locations of rare ecosystems
 33 under large amounts of anthropogenic pressure. Further, we demonstrate that verti-
 34 cal forest structural attributes which are strongly related to biodiversity via niche
 35 availability and resource partitioning are influenced negatively by anthropogenic
 36 pressures.

37 **1 Introduction**

38 A global biodiversity crisis is currently underway, driven by anthropogenic changes
 39 to natural habitats (Dirzo and Raven, 2003). Pressures such as climate change,
 40 overexploitation, and invasive species are leading to species extinctions (Thomas et
 41 al., 2004; Urban, 2015) and the homogenization of biological communities (McGill
 42 et al., 2015). The Kunming-Montreal Global Biodiversity Framework (GBF) was
 43 adopted in December 2022 with the goal of restoring and safeguarding global biodi-
 44 versity (Convention on Biological Diversity, 2023). Targets within this framework
 45 include restoring 30% of all degraded ecosystems, protecting 30% of the Earth's ter-
 46 restrial, inland water, and marine areas, and achieving no loss of high biodiversity
 47 importance areas, including high ecological integrity ecosystems (Convention on
 48 Biological Diversity, 2023). In the terrestrial environment, forest biomes have been
 49 shown to harbour the largest amount of biodiversity (Cardinale et al., 2012; Myers,
 50 1988; Pimm and Raven, 2000), and provide key ecosystem services (Thompson et
 51 al., 2009). To provide these services, it is integral that these forest ecosystems are
 52 in good ecological condition, as represented by natural or near-natural levels of for-
 53 est structure, function, and composition, often referred to as having high ecological
 54 integrity (Marín et al., 2021).

55 While understanding forest condition is a key aspect of understanding biodiversity
 56 and the provision of ecosystem services due to their inherent linkages (Cardinale et
 57 al., 2012; Hansen et al., 2021; Marín et al., 2021), it is challenging to obtain suitable
 58 field-derived data across extensive land areas due to the significant financial and
 59 temporal costs associated with large-scale field campaigns. Remote sensing data,
 60 however, can provide an efficient and cost-effective alternative to field data, offering
 61 access to new spatially explicit and comprehensive datasets that can be linked to
 62 ecological condition, with additional metrics being proposed at a rapid pace (Pereira
 63 et al., 2013; Radeloff et al., 2024; Skidmore et al., 2021). Advances in lidar technolo-

gies and modelling methods are enabling the generation of wall-to-wall estimates of forest stand structure for across entire countries (Becker et al., 2023; Matasci et al., 2018a; Matasci et al., 2018b), which serve as a more detailed indicator of ecosystem structure than the often previously used landscape fragmentation metrics (Andrew et al., 2012). Productivity metrics have been employed as a proxy for ecosystem function for many years (Pettorelli et al., 2018, 2005), with new Landsat-derived datasets providing integrative annual estimates of energy availability at a 30 m spatial resolution (Radeloff et al., 2024; Radeloff et al., 2019; Razenkova et al., n.d.). Remote sensing is quickly providing access to a vast array of datasets suitable for monitoring the various facets of biodiversity and ecological condition (Noss, 1990; Pereira et al., 2013; Skidmore et al., 2021). The integration of these datasets with information pertaining to the location of known high-ecological-integrity forests enables researchers and managers to identify high-quality forest reference states across entire jurisdictions, even in the presence of anthropogenic pressures.

Ecological reference states represent baseline conditions of ecosystems, serving as a benchmark for assessing ecological health and guiding restoration efforts (Nielsen et al., 2007). The application of counterfactual thinking, which entails considering the potential state of an ecosystem in the absence of anthropogenic pressures (Ferraro, 2009) can be instrumental for mapping high-integrity forests. Approaches such as coarsened exact matching (Iacus et al., 2012), can be used to facilitate comparisons between forest stands and their hypothetical reference states. These methods account for confounding environmental variables, thereby ensuring that all forests are compared to an appropriate reference state. Identifying a suitable reference state can be difficult, however there are methods which can be used to approximate high-integrity reference conditions. Historical reference states can be used when an ecosystem has a large depth of temporal data to compare to, however, it is not always guaranteed that an ecosystem can be restored to these historical norms due to changing climates (Balaguer et al., 2014; McNellie et al., 2020). Other proposed methods for delineating baseline conditions include protected areas (Arcese and Sinclair, 1997), and empirical estimates of the reference state generated by modelling outcomes (oftentimes species abundances and occurrence) in the absence of anthropogenic disturbance (Nielsen et al., 2007).

Protected areas, specifically designed for biodiversity conservation, are frequently faced with lower levels anthropogenic pressure as a result of biases in their placement (Joppa and Pfaff, 2009; Muise et al., 2022). In forested ecosystems, over time this leads to undisturbed high-integrity forests remaining within protected areas due to their natural disturbance regimes and a lack of anthropogenic pressures (Brumelis et al., 2011). These high-integrity forests, situated within protected areas, can serve as effective ecological baselines (Arcese and Sinclair, 1997). When suitably matched to unprotected areas, they can be used as a reference state to assess the differences between all forests and their high-integrity counterparts (Ferraro, 2009). Further, protected areas and undisturbed ecosystems such as intact forest landscapes have been shown to have increased structural densities when compared to other ecosystems (Li et al., 2023; Muise et al., 2022).

Anthropogenic pressure such as increased road densities (Nielsen et al., 2007), harvesting and fossil fuel exploration activities leading to edge effects (Bourgoin et al., 2024; Harfoot et al., 2018), and other human-induced disturbances (Liira et al., 2007) have been shown to influence forest structure. Novel datasets such as the Forest Structural Condition Index have been developed which integrate both structure and anthropogenic pressure into an index which identifies ecosystems of high conservation value, with high structural complexity and low anthropogenic pressure (Hansen et al., 2019). The impacts of anthropocentric pressure on forest functioning and energy availability is less frequently assessed. Hedwall et al. (2019) assessed plant community shifts under anthropogenic pressures in the boreal forests

of Sweden, and hypothesized that changed communities may affect forest functioning. Grantham et al. (2020) used forest extent and arrangement, alongside pressure datasets, to assess ecosystem integrity, with expectations that high-integrity ecosystems will retain high levels of ecosystem functioning. However, to our knowledge, direct impacts of anthropogenic pressures on forest ecosystem function have not been assessed at a landscape scale.

We proposed a novel, data-driven, approach to identify high-integrity forests based on various satellite-derived metrics of ecosystem condition, and calculate the degree of structural and functional similarity for unprotected areas to high-integrity forests found on Vancouver Island, British Columbia, Canada. We use a strict matching approach to ensure ecological similarity, and choose the highest 10% of metric values across variables that are known to be correlated with ecological condition and biodiversity. We then calculate ecological similarity using sigma dissimilarity (Mahony et al., 2017) alongside human footprint layers developed by Hirsh-Pearson et al. (2022) to assess the influence of anthropogenic pressure of ecological integrity by cumulative and individual pressures. Further, we compare the similarity metrics between ecological structure and function to identify linkages between ecological similarity of forest structure and forest functioning, while accounting for the presence of anthropogenic pressures.

2 Methods

2.1 Study Area

We focus on the forested areas of Vancouver Island, British Columbia, Canada. Vancouver island has approximately 31285 km² of land area, of which 79.5% is forested. The dominant forest species on Vancouver Island are Douglas-fir (*Pseudotsuga menziesii*), western red cedar (*Thuja plicata*), western hemlock (*Tsuga heterophylla*), yellow cedar (*Chamaecyparis nootkatensis*), and Sitka spruce (*Picea sitchensis*) (Burns, 1990). British Columbia generally has a temperate maritime climate, with mild, wet winters, and cool, dry summers. There are four ecosystems on Vancouver Island as defined by British Columbia's biogeoclimatic ecosystem classification (BEC) framework (Pojar et al., 1987), Coastal Western Hemlock (CWH), Mountain Hemlock (MH), Coastal Douglas Fir (CDF), and Coastal Mountain-heather Alpine (CMA), which are broadly delineated based on soil, climate, and elevation. Forestry is an important industry on Vancouver Island, while fires are historically rare and low severity (Daniels and Gray, 2006).

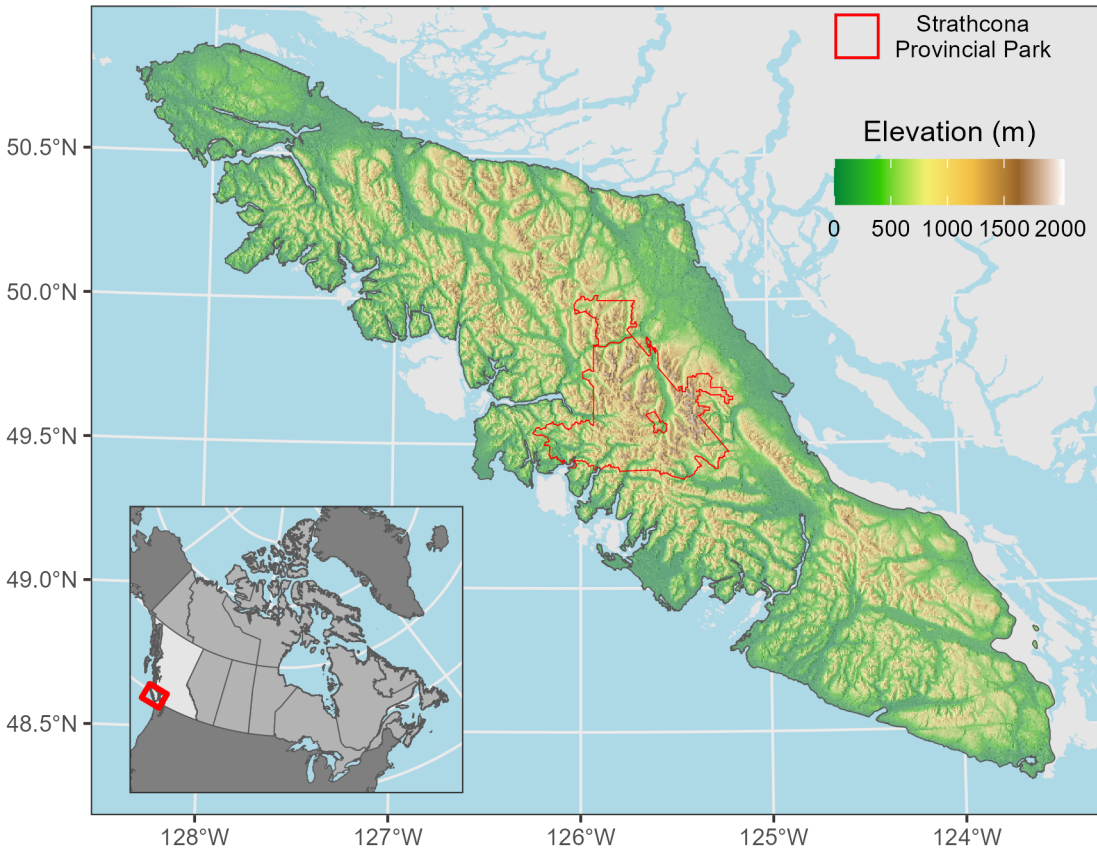


Figure 1: Study area on Vancouver Island, British Columbia, Canada, including the location of Strathcona Provincial Park.

152 2.2 Data

153 2.2.1 Reference State

154 We defined our reference state as the forested area of Strathcona Park. We chose
 155 Strathcona Park as a temporal and protected area reference state, as the oldest and
 156 largest (2480 km^2) protected area in British Columbia. Strathcona Park was estab-
 157 lished in 1911, and 80% of the park is preserved as wilderness area and designated
 158 as Nature Conservancy Areas under the *Park Act* ("Park Act," n.d.). The park con-
 159 tains three BEC zones, CWH, MH, and CMA, but does not include CDF, which
 160 is only found in the southern portion of the island. Due to this, we do not include
 161 CDF in our analysis.

2.2.2 Forest Structure

Wall-to-wall, 30 m forest structure metrics (canopy height, canopy cover, structural complexity, and aboveground biomass) were generated by Matasci et al. (2018a) for 2015 across the forested landscape of British Columbia. This data was generated by using a random forest-kNN approach, imputing airborne laser scanning derived forest structural attributes across the entirety of Canada using Landsat-derived best-available-pixel (BAP) composites (Hermosilla et al., 2016; White et al., 2014) and topographic information (Matasci et al., 2018a; Matasci et al., 2018b). The BAP composites were derived by selecting optical observations from the Landsat archive (including Landsat-5 Thematic Mapper, Landsat-7 Enhanced Thematic Mapper Plus, and Landsat-8 Operational Land Imager imagery) over the course of the growing season, considering atmospheric effects (haze, clouds, cloud shadows) and distance from the desired composite date (in this case, August 31st). Details on the pixel scoring method can be found in White et al. (2014). The BAP composites were further refined by using a spectral trend analysis on the normalized burn ratio to remove noise, and missing pixels are infilled using temporally-interpolated values. This procedure results in gap-free, surface-reflectance image composites (Hermosilla et al., 2015), which are used as the primary dataset to impute forest structural attributes (Matasci et al., 2018a; Matasci et al., 2018b).

2.2.3 Forest Function

For our forest ecosystem function dataset, we calculated the Dynamic Habitat Indices (Radeloff et al., 2019) using Landsat data on Google Earth Engine (Gorelick et al., 2017), following the methodology of Razenkova et al. (n.d.). Briefly, we created a synthetic year of NDVI composites using all available Landsat imagery from 2011-2020 (centred on 2015). We used the Landsat QA band derived from the fmask algorithm (Zhu and Woodcock, 2012) to filter out erroneous pixels, such as clouds and cloud shadows. Monthly NDVI values were calculated by taking the median of each month's NDVI observations, ignoring the year the image was acquired. This allows us to generate the DHIs at spatial resolution of 30 m, while accounting for the lower temporal resolution of the Landsat series when compared to the more commonly used MODIS satellites (Razenkova et al., n.d.). The DHIs are calculated as the sum (Cumulative DHI), minimum (Minimum DHI), and coefficient of variation (Variation DHI) of these monthly observations. The three DHIs have been shown to be indicative of biodiversity over a range of scales (Radeloff et al., 2019; Razenkova et al., 2022) and extents (Coops et al., 2019, 2009) for a variety of clades (Michaud et al., 2014; Suttidate et al., 2021). In this study, we focus on the Cumulative and Variation DHIs, as the minimum DHI is consistently 0 due to the presence of snow.

2.2.4 Anthropogenic Pressures

We use the Canadian Human Footprint as developed by Hirsh-Pearson et al. (2022). The Canadian Human Footprint is an additive pressure map generated by summing the 12 different anthropogenic pressures (built environments, crop land, pasture land, population density, nighttime lights, railways, roads, navigable waterways, dams and associated reservoirs, mining activity, oil and gas, and forestry), which ranges from zero to 55 for any cell across Canada. This cumulative dataset is also distributed with Canada-wide individual pressure values (Hirsh-Pearson et al., n.d.). Here, we focus on the overall cumulative pressure map and four individual pressures: population density, built environments, roads, and forestry. We selected these pressures as some others (oil and gas; railroads) are not present on Vancouver Island, and others, such as pasture land and crop land do not coincide with forested areas.

2.2.5 Covariates

In our matching procedure (see Section 2.3) we use two core datasets as our matching covariates. Firstly, we use a 30 m digital elevation model and derived slope dataset from the Advanced Spaceborne Thermal Emission and Reflection Radiome-

ter (ASTER) Version 2 GDEM product (Tachikawa et al., 2011). We also match on four climate variables; mean annual precipitation (MAP), mean annual temperature (MAT), mean warmest month temperature (MWMT), and mean coldest month temperature (MCMT) calculated from 1990-2020 climate normals using the ClimateNA software package at a 1 km spatial resolution, and downsampled to 30 m using cubic spline resampling in the **terra** (version 1.7-71) R package (Hijmans, 2024) in R (R Core Team, 2024 version 4.4.1). A visualization of one of each input dataset can be found in Figure Figure 2.

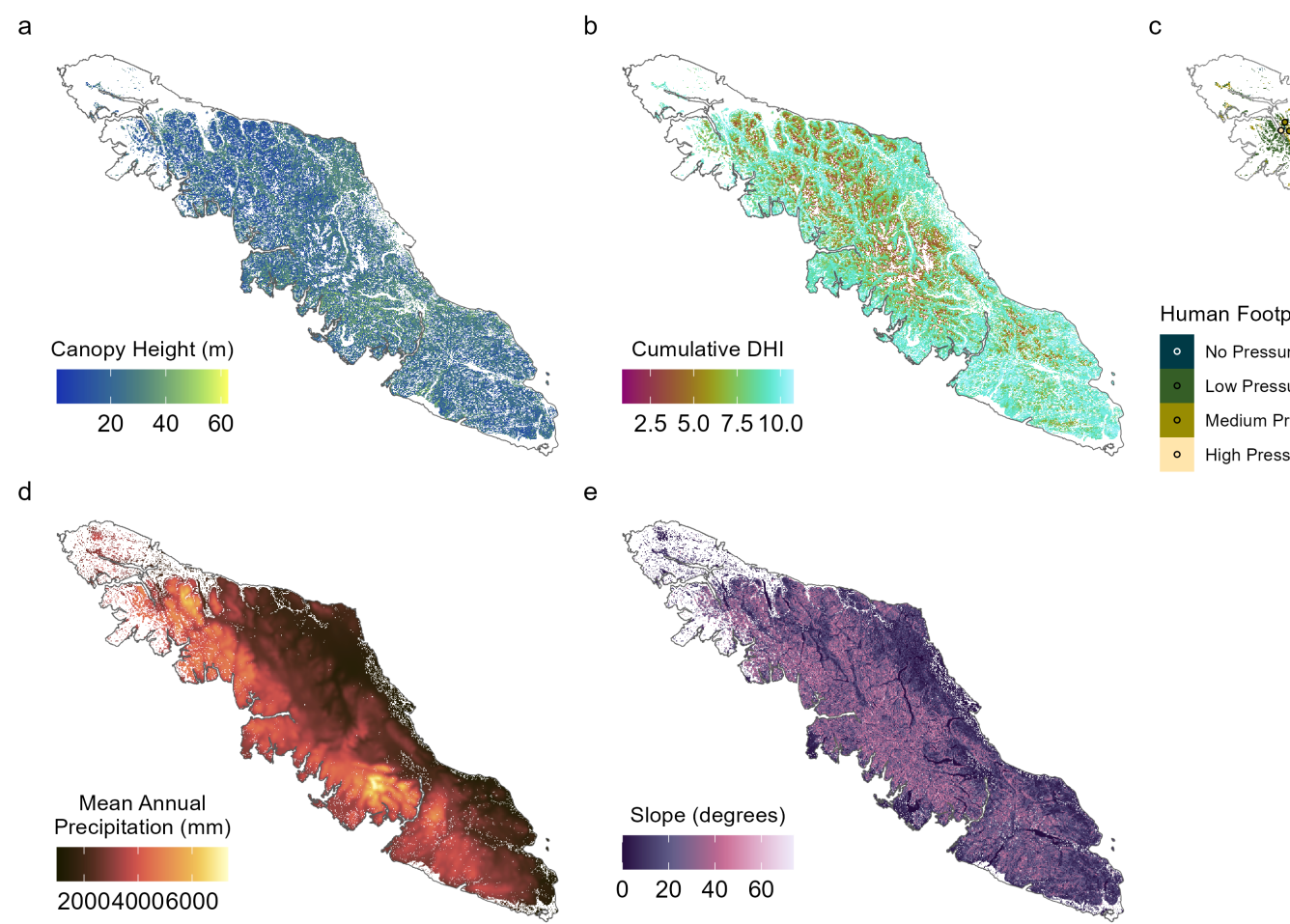


Figure 2: Visualization of the input datasets used in the study. Panel C shows the human footprint and the location of the samples used for our analysis.

223 2.3 Calculating similarity

224 We calculate the sigma dissimilarity (Mahony et al., 2017) of forested pixels across
 225 British Columbia by using an expanded coarsened exact matching (CEM) technique
 226 (Iacus et al., 2012) (Figure 3). This methodology enables us to evaluate the degree
 227 of similarity between all forested pixels in the province and natural forests, while
 228 accounting for potential confounding variables such as climate and topography. The
 229 CEM technique creates comparable groups of observations among covariates by ini-
 230 tially coarsening the covariates. In this instance, all six covariates were coarsened
 231 into five quintiles hereafter referred to as bins. CEM then performs exact matching
 232 on the bins, with each pixel matched to a climatically and topographically similar
 233 group of pixels within Strathcona Park, hereafter referred to as strata. In the case
 234 where there is not enough matched pixels found in Strathcona Park, we calculate the
 235 nearest neighbours in bin space for all strata, and sample up to 1000 pixels while
 236 minimizing the nearest neighbour distance. If the nearest neighbour distance is on
 237 average above two, we do not consider that strata in our analysis.

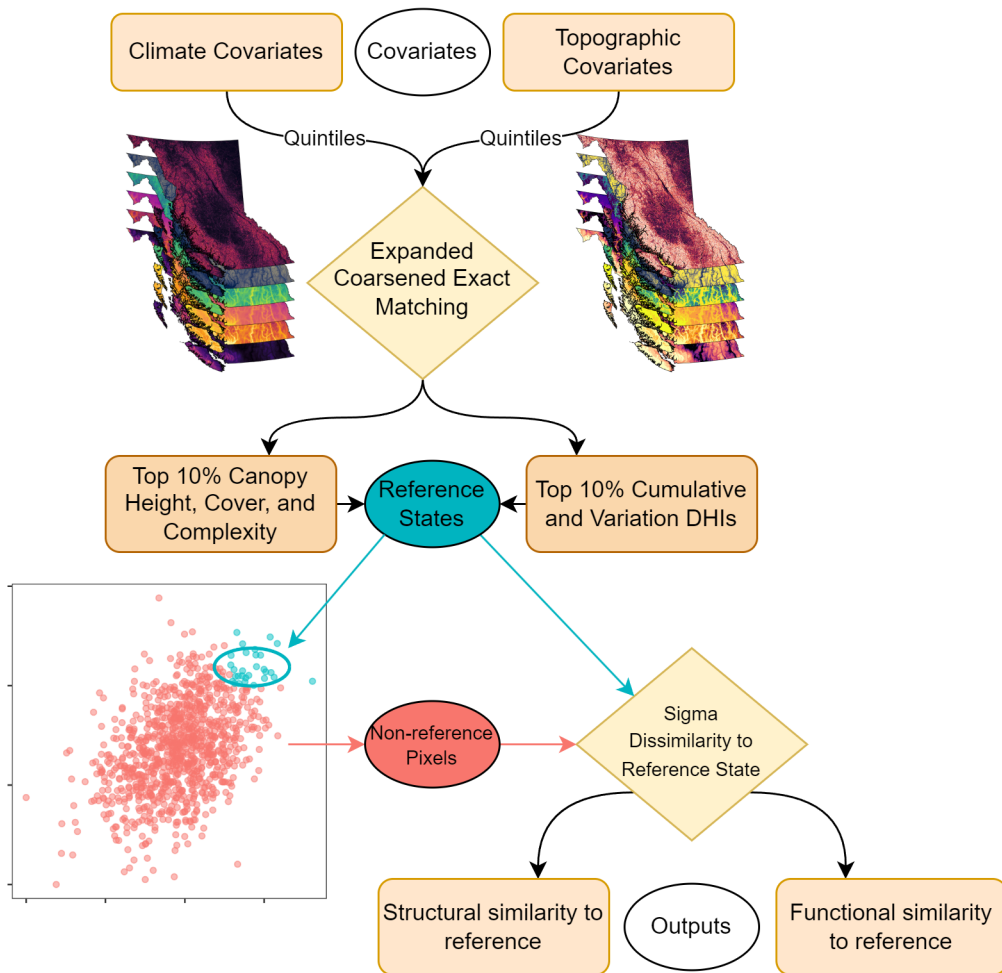


Figure 3: Conceptual flow diagram of the study.

238 Following the matching procedure, we identify data driven reference states in both
 239 structural and functional attributes by selecting the top 10% of protected, undis-
 240 turbed observations for each structural (canopy height, cover, and structural com-

plexity) and functional (cumulative and variation DHIs) attribute, separately. We then determine the similarity of all pixels, in both structural and functional attributes, to the reference states by calculating the sigma dissimilarity metric. Sigma dissimilarity standardizes the Mahalanobian distance (Mahalanobis, 1936) by rescaling it into percentiles of the chi distribution (Mahony et al., 2017). This effectively accounts for the effect of dimensionality when creating a multivariate similarity metric (Mahony et al., 2017). We calculate sigma dissimilarity for every strata with a suitable reference state, comparing all forested pixels to the top 10% of each attribute for that reference state.

2.4 Sampling

We reclassify the Canadian Human Footprint (Hirsh-Pearson et al., n.d.; Hirsh-Pearson et al., 2022) into categorical data following Hirsh-Pearson et al. (2022) and Arias-Patino et al. (2024) : a value of zero has no anthropogenic pressure, zero to four has low anthropogenic pressure, four to eight has medium anthropogenic pressure, and > eight has high anthropogenic pressure. To assess the cumulative impact of anthropogenic pressure on ecological similarity, we implement stratified sampling on all suitable strata, sampling 100 samples from each anthropogenic pressure class. For our individual pressures, we follow the same reclassification steps on each pressure layer, and sample an additional hundred samples for each pressure class. Sampling was performed using the **sgsR** (version 1.4.5) R package (Goodbody et al., 2023) with the Quiennec method (Queinnec et al., 2021). Geospatial data processing was performed using the **terra** (version 1.7-78) (Hijmans, 2024), **sf** (version 1.0-16) (Pebesma, 2018; Pebesma and Bivand, 2023), and **tidyterra** (version 0.6.1) (Hernangómez, 2023a, 2023b) R packages.

2.5 Analysis

We used a one-way analysis of variance (ANOVA) with a critical value of 0.05 to identify differences in the mean similarity values across cumulative anthropogenic pressure classes. We account for family-wise error rate for our ANOVAs using the Holm-Bonferroni method, only continuing the analysis for similarity variables with significant ANOVAs at the adjusted critical value. As ANOVAs only identify if there is a difference in means, but does not identify which means are different, we used a Tukey HSD post-hoc test to identify which means are different from the control group (no anthropogenic pressure), which also controls for the family-wise error rate.

We follow the same protocol to identify the difference in means for each anthropogenic pressure of interest (roads, population density, forestry, and built environment). We compare each pressure to the same ‘no pressure’ values sampled in the cumulative pressure analysis. All statistical analysis were conducted using the **rstatix** (version 0.7.2) R package (Kassambara, 2023).

3 Results

Our sigma dissimilarity processing workflow resulted in six island wide maps of structural and functional similarity to the reference state found in Strathcona Provincial Park (Figure 4). We display three selected subsets of Vancouver Island to demonstrate variation in similarity and the anthropogenic footprint layers. Subset A shows a region near Lake Cowichan where harvesting is a common anthropogenic pressure (Figure 4 A). Subset B shows a protected area near Campbell River with high population density (Figure 4 B). Subset C shows a region with generally low anthropogenic pressure (Figure 4 C). We see more variation in the similarity to high aboveground biomass and functional reference states, while the similarity to canopy cover, canopy height, and structural complexity is often lower across Vancouver Island.

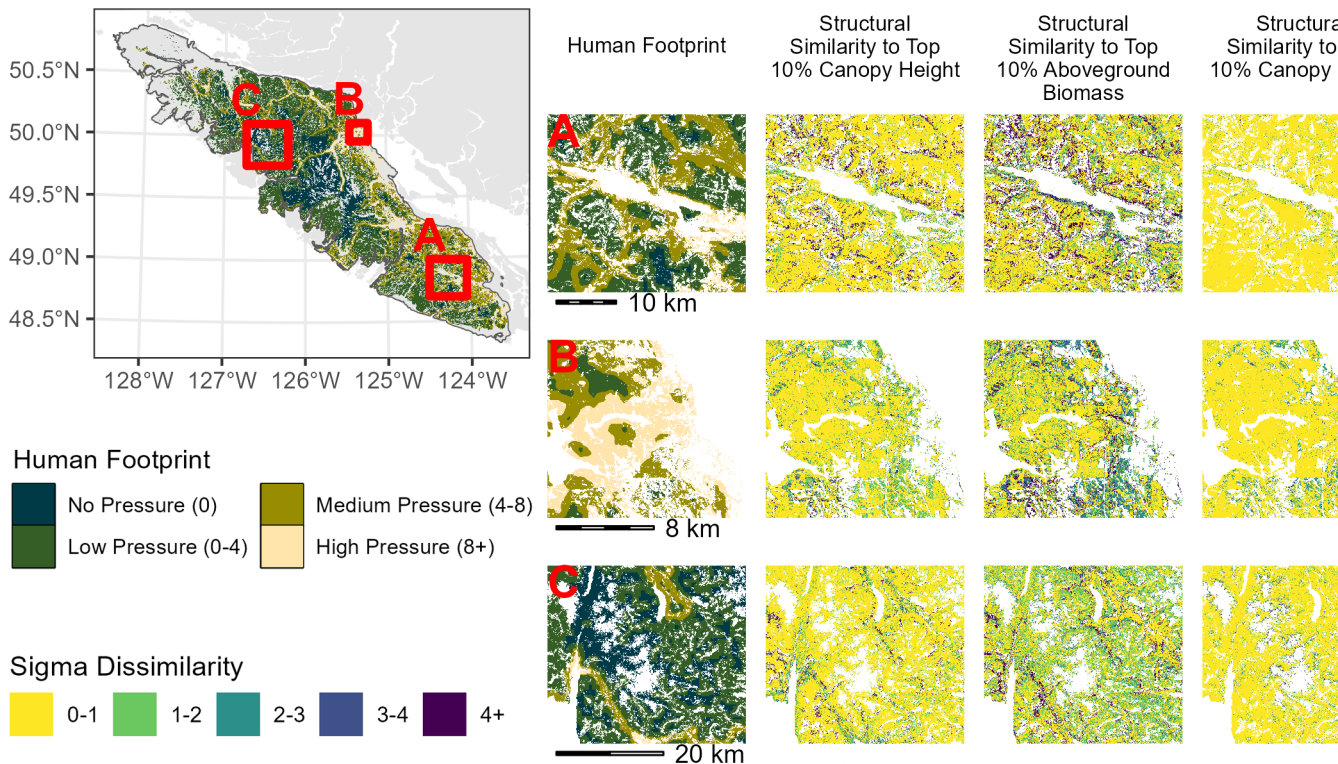


Figure 4: Regional details of the human footprint and sigma dissimilarity across the sites on Vancouver Island. Subset A show Cowichan Lake, a heavily harvested region. Subset B shows Elk Falls Provincial Park, just outside Campbell River, a region with high population density. Subset C shows a region with generally low anthropogenic pressure.

We found that similarity to high structural complexity (Anova: $p = 0.007$) and tall canopy height (Anova: $p = 0.003$) reference states was influenced by medium to high levels of cumulative anthropogenic pressure (Figure 5). Similarity to high biomass (Anova: $p = 0.142$) and canopy cover (Anova: $p = 0.855$) regions were not significantly influenced by cumulative anthropogenic pressures. Neither of the productivity metrics were influenced by cumulative anthropogenic pressures.

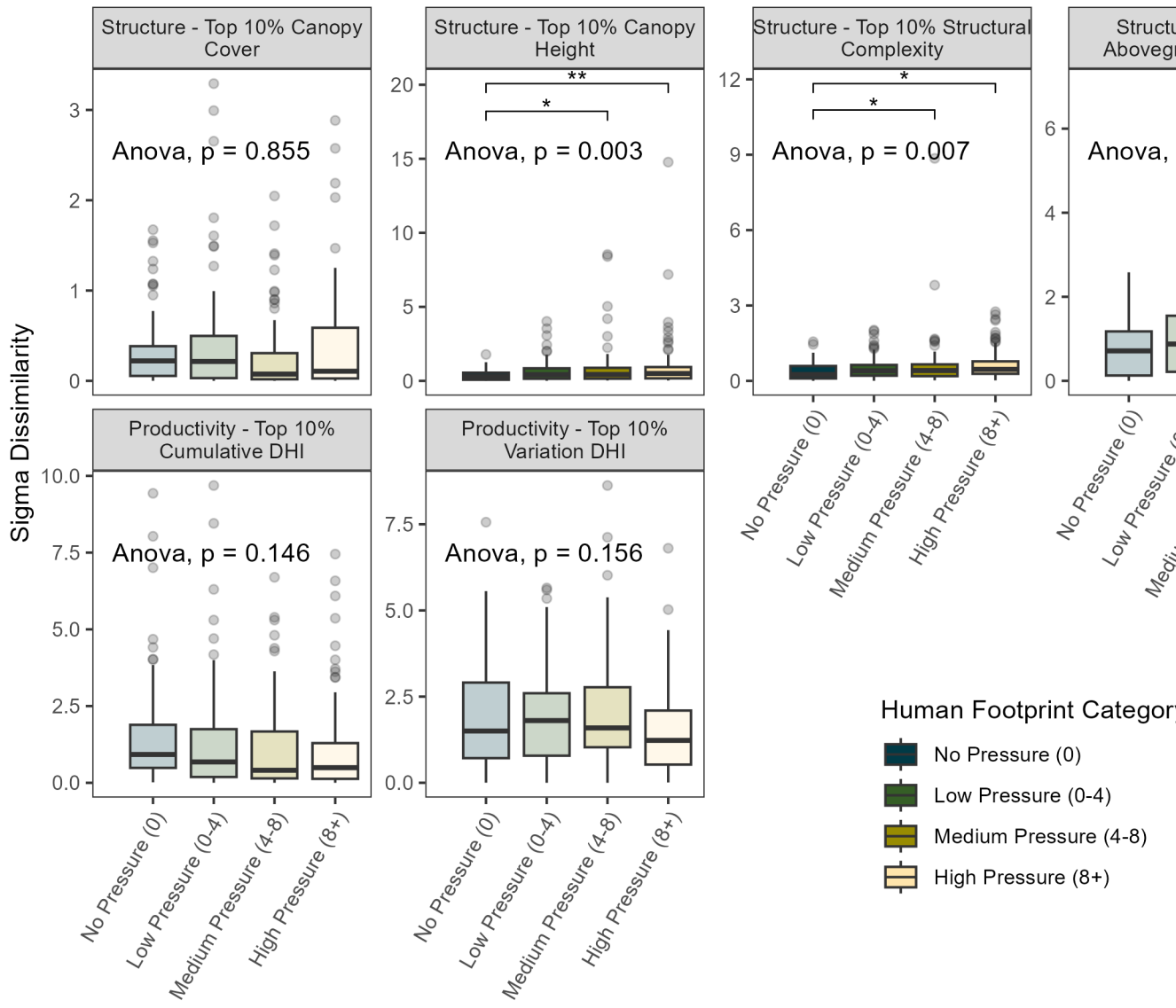


Figure 5: Boxplots of sigma similarity to the reference state in Strathcona Provincial Park by cumulative human footprint category. Anova p-values corrected using the Holm-Bonferroni method. * indicates a Tukey HSD p-value < 0.05. ** indicates a Tukey HSD p-value < 0.01.

Increases in all individual anthropogenic pressures led to increased dissimilarity when compared to most structural reference states (Figure 6). Increases in pressures from roads and built environment did not increase or reduce similarity to structural reference states with high canopy cover. Medium and high pressures from population density and forestry/harvesting increased dissimilarity to all structural reference states. Anthropogenic pressures generally did not influence the similarity to reference states based on productivity metrics, however, increases in pressures from population density decreased dissimilarity to ecosystems with high variation in energy availability.

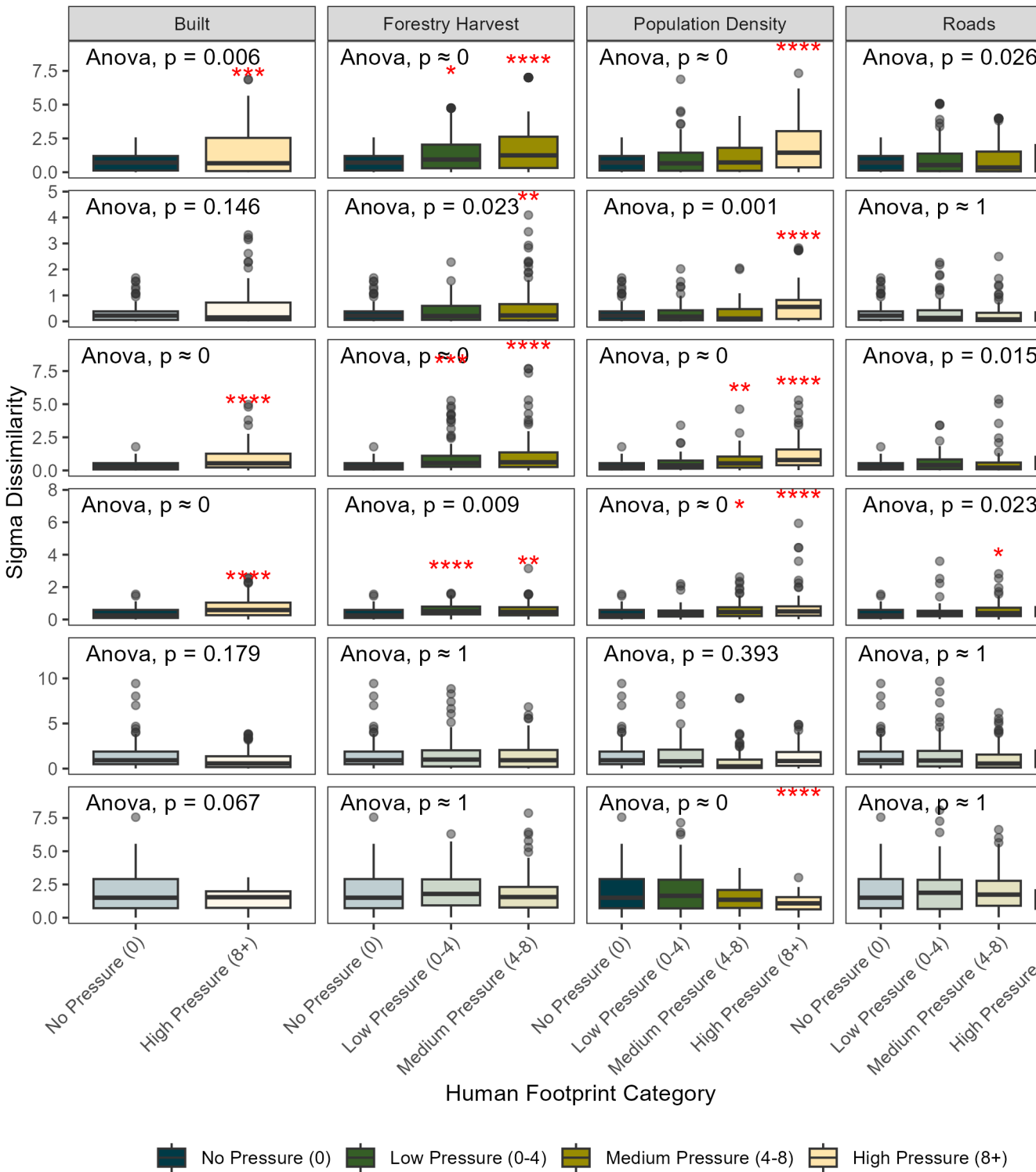


Figure 6: Boxplots of sigma similarity to the reference state in Strathcona Provincial Park by individual anthropogenic pressures. Anova p-values corrected using the Holm-Bonferroni method. * indicates a Tukey HSD p-value < 0.05. ** indicates a Tukey HSD p-value < 0.01. *** indicates a Tukey HSD p-value < 0.001. **** indicates a Tukey HSD p-value < 0.0001.

306 **4 Discussion**

307 In this paper, we use medium-resolution remote sensing metrics of ecosystem struc-
 308 ture and function to assess similarity to high-integrity forests across Vancouver
 309 Island, British Columbia. We validate our approach by assessing the influence of
 310 the human footprint on these reference states, finding that ecosystem structure in
 311 the form of forest structural attributes is influenced by increased anthropogenic
 312 pressures on a cumulative and individual level (Figure 5; Figure 6). Forest ecosys-
 313 tem function, as represented by the DHIs, is generally not significantly influenced
 314 by anthropogenic pressures, although population density increased similarity to
 315 ecosystems with high variation in energy availability (Figure 6).

316 We find that similarity to high structural complexity forests, which are often high
 317 in biodiversity due to increased niche availability (Macarthur and Macarthur, 1961;
 318 Walter et al., 2021), is impacted by medium to high levels of anthropogenic pres-
 319 sures. Structural similarity to tall forests is also impacted by medium to high levels
 320 of anthropogenic pressure, while productivity metrics were not influenced by cumula-
 321 tive anthropogenic pressures in this region (Figure 5). In tropical forests, Bourgoin
 322 et al. (2024) found that anthropogenic forest degradation influenced aboveground
 323 biomass and canopy height, however, they focus on edge effects, fire, and selective
 324 logging, rather than cumulative and individual anthropogenic pressures. Li et al.
 325 (2023) also found a global impact of anthropogenic pressures on forest structural
 326 density, however, they do not explore which facets of anthropogenic pressure are the
 327 strongest driver of forest degradation. Hansen et al. (2020) integrate forest struc-
 328 ture and anthropogenic pressure into the forest structural integrity index to identify
 329 forest stands of high ecological value (high structural quality; low anthropogenic
 330 footprint). We further this research by assessing individual pressures on a multivari-
 331 ate metric of structural similarity to a high-quality reference state (Figure 6).

332 It is possible that we did not find a relationship between cumulative anthropogenic
 333 pressures and canopy cover/aboveground biomass as these forest structural at-
 334 tributes are typically high on Vancouver Island due to the regions mild climate and
 335 suitability for forest growth (Waring et al., 2006). Conversely, we did find a rela-
 336 tionship between the vertical layering (canopy height and structural complexity) of trees
 337 and anthropogenic pressures (Figure 5). This is especially relevant as structurally
 338 complex forests are crucial for harbouring biodiversity and providing ecosystem func-
 339 tions and services. The lack of a relationship between canopy cover/aboveground
 340 biomass and the cumulative human footprint is potentially due to replanting efforts
 341 from the forestry industry following harvest, which are required in British Columbia
 342 and often lead to single species, single aged stands (Lieffers et al., 2020). Stands of
 343 this configuration are unlikely to be found in our reference state, Strathcona Provin-
 344 cial Park, as it has been a protected area for over 100 years, thus leading to higher
 345 dissimilarity values.

346 Anthropogenic effects on forest function and energy availability have rarely been
 347 examined. Here, we also examine how anthropogenic pressures influence similarity
 348 to high available energy and high energy variation forests, both hypothesized to in-
 349 dicate high levels of biodiversity in a number of guilds and clades (Radeloff et al.,
 350 2019; Razenkova et al., 2022). We do not find a strong influence of cumulative an-
 351 thropogenic pressure on our forest functioning metrics, however, we did find that
 352 similarity to forest stands with high annual energy variability was increased in high
 353 population density areas (Figure 6). This increase in similarity in high density areas
 354 is potentially driven by ornamental trees and the bias for North American urban
 355 forests to be primarily deciduous trees (Clapp et al., 2014; Roman et al., 2018),
 356 which would have a stronger variation DHI component due to annual leaf senescence
 357 and green-up.

358 Further, the calculation of the DHIs is dependent on using a vegetation index or
 359 productivity estimate, in our case NDVI. Vegetation indices have been shown to sat-
 360 urate at high levels of canopy cover and leaf area index (Huete et al., 2002; Huete et
 361 al., 1997), which are common on Vancouver Island, and comparisons of unprotected
 362 areas to the highest 10% cover in reference states shows no significant difference
 363 (Figure 5). Recent research has shown that seasonality, here represented as the Vari-
 364 ation DHI, drives functional diversity in avian assemblages, however, these results
 365 also strongly varied by region (Keyser et al., 2024). It is possible that examining
 366 anthropogenic pressure impacts in regions with more variation in canopy cover
 367 may lead to differing results depending on the amount of total variation present in
 368 canopy cover, which would in turn influence seasonality and energy availability.

369 Assessing individual pressure influences on the environment is also relevant to ques-
 370 tions of how cumulative anthropogenic pressure maps are calculate. There is cur-
 371 rently a debate between additive and antagonistic anthropogenic pressure mapping
 372 methods, as there is little information on mechanistic interactions between pressures
 373 (Arias-Patino et al., 2024). We assess individual pressures on structural and func-
 374 tional similarity in forests across Vancouver Island, Canada, an advancement upon
 375 the current standard of using a single value of cumulative anthropogenic pressure
 376 (Bourgoin et al., 2024; Li et al., 2023). Similar methods could be used to examine
 377 mechanistic pressure interactions across large scales.

378 We apply the Sigma Dissimilarity metric developed by Mahony et al. (2017) to de-
 379 termine similarity to high-integrity ecosystems, and use a matching approach to
 380 account for environmental covariates. This method accounts for the multidimes-
 381 sionality of the structure and function datasets, and standardizes them so they are
 382 comparable. This is especially relevant in our case as we use four forest structural
 383 attributes and two forest function metrics. These methods are similar to other simi-
 384 larity metrics commonly applied in remote sensing for multivariate similarity such as
 385 spectral similarity (Schweiger et al., 2018), and phenospectral similarity (Osei Darko
 386 et al., 2024).

387 While we are limited in number of structural variables due to the imputation of the
 388 lidar-derived dataset across the study area (Matasci et al., 2018a; Matasci et al.,
 389 2018b), future studies could directly use raw lidar datasets to create a multitude of
 390 metrics, and apply the sigma similarity method to those. This could capture addi-
 391 tional facets of similarity which are missed when using a Canada-wide dataset with
 392 limited forest structural attributes at 30 m. New spaceborne lidar missions such as
 393 GEDI (Dubayah et al., 2020) and IceSAT-II (Neumann et al., 2019) are also pro-
 394 viding estimates of forest structure across the globe. However, these satellites are
 395 sample based missions, and do not provide wall-to-wall coverage (Duncanson et al.,
 396 2021).

397 We assess multiple definitions of high quality forest across a large region using a
 398 data-driven approach. Often, it is common for reference states to be unavailable
 399 due to a lack of data on regions of high ecological integrity, especially across large
 400 regions (McNellie et al., 2020). We attempt to circumvent this by using a large,
 401 long-established protected area (Strathcona Provincial Park; Figure 1), and a match-
 402 ing technique that preserves ecological similarity between reference states and their
 403 counterparts. The long-established, large protected area ensures that little anthro-
 404 pogenic pressures or modification have been made to the landscape, while also guar-
 405 anteeing that the reference state is attainable for a given topography and climate
 406 (Corlett, 2016; Hobbs et al., 2014) due to contemporary nature of the reference
 407 state. Our matching technique (coarsened exact matching, combined with an kNN
 408 approach when no exact match is available) allows us to generate reference states
 409 in a near wall-to-wall fashion, which ensures similarity between reference state and
 410 compared pixels.

Our techniques move beyond traditional impact evaluation techniques (Ferraro, 2009) commonly used in protected area effectiveness assessments by allowing spatial reconstruction of conservation outcomes, and generating a multivariate, rather than univariate, assessment of similarity to high ecological integrity forests. While our methods in this paper use a data-driven approach to derive reference states, if an individual or organization is interested in a specific species or ecosystem, and has known locations of high quality ecosystems associated with that species or ecosystem, these methods can be applied to assess similarity to those high quality ecosystems across large regions.

5 Acknowledgements

This research was funded by NSERC support of Coops (RGPIN-2024-04402). Remote sensing data products used in this research are free and open and available for download at https://ca.nfis.org/maps_eng.html. The authors thank Dr. Michael A. Wulder and Dr. Joanne C. White for development and early access to these National Terrestrial Ecosystem Mapping System (NTEMS) products. They thank Dr. Elena Razenkova for early access to the Landsat-derived Dynamic Habitat Indices. ERM would like to thank the members of the IRSS for many helpful conversations throughout the preparation of this manuscript.

6 Ethics

The authors declare no conflicts of interest.

References

- Andrew, M.E., Wulder, M.A., Coops, N.C., 2012. Identification of *de facto* protected areas in boreal Canada. Biological Conservation 146, 97–107. <https://doi.org/10.1016/j.biocon.2011.11.029>
- Arcese, P., Sinclair, A.R.E., 1997. The role of protected areas as ecological baselines. The Journal of Wildlife Management 61, 587–602. <https://doi.org/10.2307/3802167>
- Arias-Patino, M., Johnson, C.J., Schuster, R., Wheate, R.D., Venter, O., 2024. Accuracy, uncertainty, and biases in cumulative pressure mapping. Ecological Indicators 166, 112407. <https://doi.org/10.1016/j.ecolind.2024.112407>
- Balaguer, L., Escudero, A., Martín-Duque, J.F., Mola, I., Aronson, J., 2014. The historical reference in restoration ecology: Re-defining a cornerstone concept. Biological Conservation 176, 12–20. <https://doi.org/10.1016/j.biocon.2014.05.007>
- Becker, A., Russo, S., Puliti, S., Lang, N., Schindler, K., Wegner, J.D., 2023. Country-wide retrieval of forest structure from optical and SAR satellite imagery with deep ensembles. ISPRS Journal of Photogrammetry and Remote Sensing 195, 269–286. <https://doi.org/10.1016/j.isprsjprs.2022.11.011>
- Bourgoin, C., Ceccherini, G., Girardello, M., Vancutsem, C., Avitabile, V., Beck, P.S.A., Beuchle, R., Blanc, L., Duveiller, G., Migliavacca, M., Vieilledent, G., Cescatti, A., Achard, F., 2024. Human degradation of tropical moist forests is greater than previously estimated. Nature 631, 570–576. <https://doi.org/10.1038/s41586-024-07629-0>
- Brumelis, G., Jonsson, B.G., Kouki, J., Kuuluvainen, T., Shorohova, E., 2011. Forest naturalness in northern Europe: perspectives on processes, structures and species diversity. Silva Fennica 45.
- Burns, R.M., 1990. Silvics of North America. U.S. Department of Agriculture, Forest Service.
- Cardinale, B.J., Duffy, J.E., Gonzalez, A., Hooper, D.U., Perrings, C., Venail, P., Narwani, A., Mace, G.M., Tilman, D., Wardle, D.A., Kinzig, A.P., Daily, G.C., Loreau, M., Grace, J.B., Larigauderie, A., Srivastava, D.S., Naeem, S., 2012.

- 462 Biodiversity loss and its impact on humanity. *Nature* 486, 59–67. <https://doi.org/10.1038/nature11148>
- 463
- 464 Clapp, J.C., Ryan III, H.D.P., Harper, R.W., Bloniarz, D.V., 2014. Rationale for the
465 increased use of conifers as functional green infrastructure: A literature review
466 and synthesis. *Arboricultural Journal* 36, 161–178. <https://doi.org/10.1080/03071375.2014.950861>
- 467
- 468 Convention on Biological Diversity, 2023. Report of the conference of the parties to
469 the Convention on Biological Diversity on the second part of its fifteenth meeting
470 (No. CBD/COP/15/17).
- 471 Coops, N.C., Bolton, D.K., Hobi, M.L., Radeloff, V.C., 2019. Untangling multiple
472 species richness hypothesis globally using remote sensing habitat indices. *Ecological
473 Indicators* 107. <https://doi.org/10.1016/j.ecolind.2019.105567>
- 474 Coops, N.C., Waring, R.H., Wulder, M.A., Pidgeon, A.M., Radeloff, V.C., 2009.
475 Bird diversity: A predictable function of satellite-derived estimates of seasonal
476 variation in canopy light absorbance across the united states. *JOURNAL OF
477 BIOGEOGRAPHY* 36, 905–918. <https://doi.org/10.1111/j.1365-2699.2008.02053.x>
- 478
- 479 Corlett, R.T., 2016. Restoration, reintroduction, and rewilding in a changing world.
480 *Trends in Ecology & Evolution* 31, 453–462. <https://doi.org/10.1016/j.tree.2016.02.017>
- 481
- 482 Daniels, L.D., Gray, R.W., 2006. Disturbance regimes in coastal British Columbia.
483 *Journal of Ecosystems and Management* 7. <https://doi.org/10.22230/jem.2006v7n2a542>
- 484
- 485 Dirzo, R., Raven, P.H., 2003. Global State of Biodiversity and Loss. Annual Re-
486 view of Environment and Resources 28, 137–167. <https://doi.org/10.1146/annurev.energy.28.050302.105532>
- 487
- 488 Dubayah, R., Blair, J.B., Goetz, S., Fatoyinbo, L., Hansen, M., Healey, S., Hofton,
489 M., Hurt, G., Kellner, J., Luthcke, S., Armston, J., Tang, H., Duncanson, L.,
490 Hancock, S., Jantz, P., Marselis, S., Patterson, P.L., Qi, W., Silva, C., 2020.
491 The Global Ecosystem Dynamics Investigation: High-resolution laser ranging
492 of the Earth's forests and topography. *Science of Remote Sensing* 1, 100002.
493 <https://doi.org/10.1016/j.srs.2020.100002>
- 494
- 495 Duncanson, L., Neuenschwander, A., Silva, C.A., Montesano, P., Guenther, E.,
496 Thomas, N., Hancock, S., Minor, D., White, J., Wulder, M., Armston, J., 2021.
497 2021 IEEE international geoscience and remote sensing symposium IGARSS. pp.
498 670–672. <https://doi.org/10.1109/IGARSS47720.2021.9553209>
- 499
- 500 Ferraro, P.J., 2009. Counterfactual thinking and impact evaluation in environmental
501 policy. *New Directions for Evaluation* 2009, 75–84. <https://doi.org/10.1002/ev.297>
- 501
- 502 Goodbody, T.R.H., Coops, N.C., Queinnec, M., White, J.C., Tompalski, P., Hudak,
503 A.T., Auty, D., Valbuena, R., LeBoeuf, A., Sinclair, I., McCartney, G., Prieur,
504 J.-F., Woods, M.E., 2023. sgsR: A structurally guided sampling toolbox for
505 LiDAR-based forest inventories. *Forestry: An International Journal of Forest
Research* cpac055. <https://doi.org/10.1093/forestry/cpac055>
- 506
- 507 Gorelick, N., Hancher, M., Dixon, M., Ilyushchenko, S., Thau, D., Moore, R., 2017.
508 Google Earth Engine: Planetary-scale geospatial analysis for everyone. *Remote
Sensing of Environment, Big Remotely Sensed Data: tools, applications and
experiences* 202, 18–27. <https://doi.org/10.1016/j.rse.2017.06.031>
- 509
- 510 Grantham, H.S., Duncan, A., Evans, T.D., Jones, K.R., Beyer, H.L., Schuster,
511 R., Walston, J., Ray, J.C., Robinson, J.G., Callow, M., Clements, T., Costa,
512 H.M., DeGennmis, A., Elsen, P.R., Ervin, J., Franco, P., Goldman, E., Goetz,
513 S., Hansen, A., Hofsvang, E., Jantz, P., Jupiter, S., Kang, A., Langhammer, P.,
514 Laurance, W.F., Lieberman, S., Linkie, M., Malhi, Y., Maxwell, S., Mendez,
515 M., Mittermeier, R., Murray, N.J., Possingham, H., Radachowsky, J., Saatchi,
516 S., Samper, C., Silverman, J., Shapiro, A., Strassburg, B., Stevens, T., Stokes,

- 517 E., Taylor, R., Tear, T., Tizard, R., Venter, O., Visconti, P., Wang, S., Watson, J.E.M., 2020. Anthropogenic modification of forests means only 40. *Nature Communications* 11, 5978. <https://doi.org/10.1038/s41467-020-19493-3>
- 518 Hansen, A., Barnett, K., Jantz, P., Phillips, L., Goetz, S.J., Hansen, M., Venter, O., Watson, J.E.M., Burns, P., Atkinson, S., Rodríguez-Buriticá, S., Ervin, J., Virnig, A., Supples, C., De Camargo, R., 2019. Global humid tropics forest structural condition and forest structural integrity maps. *Scientific Data* 6, 232. <https://doi.org/10.1038/s41597-019-0214-3>
- 519 Hansen, A.J., Burns, P., Ervin, J., Goetz, S.J., Hansen, M., Venter, O., Watson, J.E.M., Jantz, P.A., Virnig, A.L.S., Barnett, K., Pillay, R., Atkinson, S., Supples, C., Rodríguez-Buriticá, S., Armenteras, D., 2020. A policy-driven framework for conserving the best of Earth's remaining moist tropical forests. *Nature Ecology & Evolution* 4, 1377–1384. <https://doi.org/10.1038/s41559-020-1274-7>
- 520 Hansen, A.J., Noble, B.P., Veneros, J., East, A., Goetz, S.J., Supples, C., Watson, J.E.M., Jantz, P.A., Pillay, R., Jetz, W., Ferrier, S., Grantham, H.S., Evans, T.D., Ervin, J., Venter, O., Virnig, A.L.S., 2021. Toward monitoring forest ecosystem integrity within the post-2020 Global Biodiversity Framework. *Conservation Letters* 14, e12822. <https://doi.org/10.1111/conl.12822>
- 521 Harfoot, M.B.J., Tittensor, D.P., Knight, S., Arnell, A.P., Blyth, S., Brooks, S., Butchart, S.H.M., Hutton, J., Jones, M.I., Kapos, V., Scharlemann, J.P.W., Burgess, N.D., 2018. Present and future biodiversity risks from fossil fuel exploitation. *Conservation Letters* 11, e12448. <https://doi.org/10.1111/conl.12448>
- 522 Hedwall, P.-O., Gustafsson, L., Brunet, J., Lindbladh, M., Axelsson, A.-L., Stengbom, J., 2019. Half a century of multiple anthropogenic stressors has altered northern forest understory plant communities. *ECOLOGICAL APPLICATIONS* 29, e01874. <https://doi.org/10.1002/eap.1874>
- 523 Hermosilla, T., Wulder, M.A., White, J.C., Coops, N.C., Hobart, G.W., 2015. An integrated landsat time series protocol for change detection and generation of annual gap-free surface reflectance composites. *Remote Sensing of Environment* 158, 220234. <https://doi.org/10.1016/j.rse.2014.11.005>
- 524 Hermosilla, T., Wulder, M.A., White, J.C., Coops, N.C., Hobart, G.W., Campbell, L.B., 2016. Mass data processing of time series landsat imagery: Pixels to data products for forest monitoring. *International Journal of Digital Earth* 9, 10351054. <https://doi.org/10.1080/17538947.2016.1187673>
- 525 Hernangómez, D., 2023a. Using the tidyverse with terra objects: the tidyterra package. *Journal of Open Source Software* 8, 5751. <https://doi.org/10.21105/joss.05751>
- 526 Hernangómez, D., 2023b. Using the tidyverse with terra objects: The tidyterra package. *Journal of Open Source Software* 8, 5751. <https://doi.org/10.21105/joss.05751>
- 527 Hijmans, R.J., 2024. *Terra: Spatial data analysis*.
- 528 Hirsh-Pearson, K., Johnson, C.J., Schuster, R., Wheate, R.D., Venter, O., 2022. Canada's human footprint reveals large intact areas juxtaposed against areas under immense anthropogenic pressure. *FACETS* 7, 398–419. <https://doi.org/10.1139/facets-2021-0063>
- 529 Hirsh-Pearson, K., Johnson, C., Schuster, R., Wheate, R., Venter, O., n.d. The Canadian Human Footprint. <https://doi.org/10.5683/SP2/EVKAVL>
- 530 Hobbs, R.J., Higgs, E., Hall, C.M., Bridgewater, P., Chapin III, F.S., Ellis, E.C., Ewel, J.J., Hallett, L.M., Harris, J., Hulvey, K.B., Jackson, S.T., Kennedy, P.L., Kueffer, C., Lach, L., Lantz, T.C., Lugo, A.E., Mascaro, J., Murphy, S.D., Nelson, C.R., Perring, M.P., Richardson, D.M., Seastedt, T.R., Standish, R.J., Starzomski, B.M., Suding, K.N., Tognetti, P.M., Yakob, L., Yung, L., 2014. Managing the whole landscape: historical, hybrid, and novel ecosystems. *Frontiers in Ecology and the Environment* 12, 557–564. <https://doi.org/10.1890/130300>

- 572 Huete, A., Didan, K., Miura, T., Rodriguez, E.P., Gao, X., Ferreira, L.G., 2002.
 573 Overview of the radiometric and biophysical performance of the MODIS vegeta-
 574 tion indices. *Remote Sensing of Environment* 83, 195–213. [https://doi.org/10.1016/S0034-4257\(02\)00096-2](https://doi.org/10.1016/S0034-4257(02)00096-2)
- 575 Huete, A.R., Liu, H., Leeuwen, W.J.D. van, 1997. IGARSS'97. 1997 IEEE in-
 576 ternational geoscience and remote sensing symposium proceedings. *Remote*
 577 *sensing - a scientific vision for sustainable development.* pp. 1966–1968 vol.4.
 578 <https://doi.org/10.1109/IGARSS.1997.609169>
- 580 Iacus, S.M., King, G., Porro, G., 2012. Causal Inference without Balance Check-
 581 ing: Coarsened Exact Matching. *Political Analysis* 20, 1–24. <https://doi.org/10.1093/pan/mpr013>
- 583 Joppa, L.N., Pfaff, A., 2009. High and Far: Biases in the Location of Protected Ar-
 584 eas. *PLOS ONE* 4, e8273. <https://doi.org/10.1371/journal.pone.0008273>
- 585 Kassambara, A., 2023. *Rstatix: Pipe-friendly framework for basic statistical tests.*
- 586 Keyser, S.R., Pauli, J.N., Fink, D., Radeloff, V.C., Pigot, A.L., Zuckerberg, B.,
 587 2024. Seasonality Structures Avian Functional Diversity and Niche Packing
 588 Across North America. *Ecology Letters* 27, e14521. <https://doi.org/10.1111/ele.14521>
- 590 Li, W., Guo, W.-Y., Pasgaard, M., Niu, Z., Wang, L., Chen, F., Qin, Y., Svenning,
 591 J.-C., 2023. Human fingerprint on structural density of forests globally. *Nature*
 592 *Sustainability* 6, 368–379. <https://doi.org/10.1038/s41893-022-01020-5>
- 593 Lieffers, V.J., Pinno, B.D., Beverly, J.L., Thomas, B.R., Nock, C., 2020. Refor-
 594 estation policy has constrained options for managing risks on public forests.
 595 *Canadian Journal of Forest Research* 50, 855–861. <https://doi.org/10.1139/cjfr-2019-0422>
- 597 Liira, J., Sepp, T., Parrest, O., 2007. The forest structure and ecosystem quality
 598 in conditions of anthropogenic disturbance along productivity gradient. *Forest*
 599 *Ecology and Management, Disturbances at multiple scales as the basis of forest*
 600 *ecosystem restoration and management* 250, 34–46. <https://doi.org/10.1016/j.foreco.2007.03.007>
- 602 MacArthur, R., MacArthur, J., 1961. On bird species-diversity. *Ecology* 42, 594– &
 603 <https://doi.org/10.2307/1932254>
- 604 Mahalanobis, P.C., 1936. On the generalized distance in statistics. *Proceedings of*
 605 *the National Institute of Sciences (Calcutta)* 2, 4955.
- 606 Mahony, C.R., Cannon, A.J., Wang, T., Aitken, S.N., 2017. A closer look at novel
 607 climates: new methods and insights at continental to landscape scales. *Global*
 608 *Change Biology* 23, 3934–3955. <https://doi.org/10.1111/gcb.13645>
- 609 Marín, A.I., Abdul Malak, D., Bastrup-Birk, A., Chirici, G., Barbuti, A., Kleeschulte,
 610 S., 2021. Mapping forest condition in europe: Methodological developments in
 611 support to forest biodiversity assessments. *Ecological Indicators* 128, 107839.
 612 <https://doi.org/10.1016/j.ecolind.2021.107839>
- 613 Matasci, G., Hermosilla, T., Wulder, M.A., White, J.C., Coops, N.C., Hobart, G.W.,
 614 Bolton, D.K., Tompalski, P., Bater, C.W., 2018a. Three decades of forest struc-
 615 tural dynamics over canada's forested ecosystems using landsat time-series and
 616 lidar plots. *Remote Sensing of Environment* 216, 697714. <https://doi.org/10.1016/j.rse.2018.07.024>
- 618 Matasci, G., Hermosilla, T., Wulder, M.A., White, J.C., Coops, N.C., Hobart, G.W.,
 619 Zald, H.S.J., 2018b. Large-area mapping of Canadian boreal forest cover, height,
 620 biomass and other structural attributes using Landsat composites and lidar
 621 plots. *Remote Sensing of Environment* 209, 90–106. <https://doi.org/10.1016/j.rse.2017.12.020>
- 623 McGill, B.J., Dornelas, M., Gotelli, N.J., Magurran, A.E., 2015. Fifteen forms of bio-
 624 diversity trend in the Anthropocene. *Trends in Ecology & Evolution* 30, 104–113.
 625 <https://doi.org/10.1016/j.tree.2014.11.006>

- 626 McNellie, M.J., Oliver, I., Dorrough, J., Ferrier, S., Newell, G., Gibbons, P., 2020.
 627 Reference state and benchmark concepts for better biodiversity conservation
 628 in contemporary ecosystems. *Global Change Biology* 26, 6702–6714. <https://doi.org/10.1111/gcb.15383>
- 629 Michaud, J.-S., Coops, N.C., Andrew, M.E., Wulder, M.A., Brown, G.S., Rickbeil,
 630 G.J.M., 2014. Estimating moose (*alces alces*) occurrence and abundance from
 631 remotely derived environmental indicators. *REMOTE SENSING OF ENVIRON-
 632 MENT* 152, 190–201. <https://doi.org/10.1016/j.rse.2014.06.005>
- 633 Muise, E.R., Coops, N.C., Hermosilla, T., Ban, S.S., 2022. Assessing representation
 634 of remote sensing derived forest structure and land cover across a network of
 635 protected areas. *Ecological Applications* 32, e2603. <https://doi.org/10.1002/eap.2603>
- 636 Myers, N., 1988. Threatened biotas: "Hot spots" in tropical forests. *Environmental-
 637 ist* 8, 187–208. <https://doi.org/10.1007/BF02240252>
- 638 Neumann, T.A., Martino, A.J., Markus, T., Bae, S., Bock, M.R., Brenner, A.C.,
 639 Brunt, K.M., Cavanaugh, J., Fernandes, S.T., Hancock, D.W., Harbeck, K., Lee,
 640 J., Kurtz, N.T., Luers, P.J., Luthcke, S.B., Magruder, L., Pennington, T.A.,
 641 Ramos-Izquierdo, L., Rebeld, T., Skoog, J., Thomas, T.C., 2019. The Ice, Cloud,
 642 and Land Elevation Satellite – 2 mission: A global geolocated photon product de-
 643 rived from the Advanced Topographic Laser Altimeter System. *Remote Sensing
 644 of Environment* 233, 111325. <https://doi.org/10.1016/j.rse.2019.111325>
- 645 Nielsen, S.E., Bayne, E.M., Schieck, J., Herbers, J., Boutin, S., 2007. A new method
 646 to estimate species and biodiversity intactness using empirically derived reference
 647 conditions. *Biological Conservation* 137, 403–414. <https://doi.org/10.1016/j.biocon.2007.02.024>
- 648 Noss, R.F., 1990. Indicators for Monitoring Biodiversity: A Hierarchical Approach.
 649 *Conservation Biology* 4, 355–364. <https://doi.org/10.1111/j.1523-1739.1990.tb00309.x>
- 650 Osei Darko, P., Laliberté, E., Kalacska, M., Arroyo-Mora, J.P., Gonzalez, A., Zu-
 651 loaga, J., 2024. Phenospectral similarity as an index of ecological integrity. *Fron-
 652 tiers in Environmental Science* 12. <https://doi.org/10.3389/fenvs.2024.1333762>
- 653 Park Act, n.d. RSBC 1996, c 344.
- 654 Pebesma, E., 2018. Simple Features for R: Standardized Support for Spatial Vector
 655 Data. *The R Journal* 10, 439–446. <https://doi.org/10.32614/RJ-2018-009>
- 656 Pebesma, E., Bivand, R., 2023. Spatial Data Science: With applications in R. Chapman
 657 and Hall/CRC. <https://doi.org/10.1201/9780429459016>
- 658 Pereira, H.M., Ferrier, S., Walters, M., Geller, G.N., Jongman, R.H.G., Scholes, R.J.,
 659 Bruford, M.W., Brummitt, N., Butchart, S.H.M., Cardoso, A.C., Coops, N.C.,
 660 Dulloo, E., Faith, D.P., Freyhof, J., Gregory, R.D., Heip, C., Hoft, R., Hurt, G., Jetz, W., Karp, D.S., McGeoch, M.A., Obura, D., Onoda, Y., Pettorelli, N., Reyers, B., Sayre, R., Scharlemann, J.P.W., Stuart, S.N., Turak, E., Walpole, M., Wegmann, M., 2013. Essential Biodiversity Variables. *Science* 339, 277–278. <https://doi.org/10.1126/science.1229931>
- 661 Pettorelli, N., Schulte to Bühne, H., Tulloch, A., Dubois, G., Macinnis-Ng, C., Queirós, A.M., Keith, D.A., Wegmann, M., Schrot, F., Stellmes, M., Sonnenchein, R., Geller, G.N., Roy, S., Somers, B., Murray, N., Bland, L., Geijzendorffer, I., Kerr, J.T., Broszeit, S., Leitão, P.J., Duncan, C., El Seray, G., He, K.S., Blanchard, J.L., Lucas, R., Mairoti, P., Webb, T.J., Nicholson, E., 2018. Satellite remote sensing of ecosystem functions: opportunities, challenges and way forward. *Remote Sensing in Ecology and Conservation* 4, 71–93. <https://doi.org/10.1002/rse2.59>
- 662 Pettorelli, N., Vik, J.O., Mysterud, A., Gaillard, J.-M., Tucker, C.J., Stenseth, N.Ch., 2005. Using the satellite-derived NDVI to assess ecological responses

- 680 to environmental change. Trends in Ecology & Evolution 20, 503–510. <https://doi.org/10.1016/j.tree.2005.05.011>
- 681 Pimm, S.L., Raven, P., 2000. Extinction by numbers. Nature 403, 843–845. <https://doi.org/10.1038/35002708>
- 682 Pojar, J., Klinka, K., Meidinger, D.V., 1987. Biogeoclimatic ecosystem classifi-
683 cation in British Columbia. Forest Ecology and Management 22, 119–154.
[https://doi.org/10.1016/0378-1127\(87\)90100-9](https://doi.org/10.1016/0378-1127(87)90100-9)
- 684 Queinnec, M., White, J.C., Coops, N.C., 2021. Comparing airborne and spaceborne
685 photon-counting LiDAR canopy structural estimates across different boreal for-
686 est types. Remote Sensing of Environment 262, 112510. <https://doi.org/10.1016/j.rse.2021.112510>
- 687 R Core Team, 2024. **R: A language and environment for statistical computing.** R
688 Foundation for Statistical Computing, Vienna, Austria.
- 689 Radeloff, V.C., Dubinin, M., Coops, N.C., Allen, A.M., Brooks, T.M., Clayton,
690 M.K., Costa, G.C., Graham, C.H., Helmers, D.P., Ives, A.R., Kolesov, D., Pid-
691 geon, A.M., Rapacciulo, G., Razenkova, E., Suttidate, N., Young, B.E., Zhu, L.,
692 Hobi, M.L., 2019. The Dynamic Habitat Indices (DHIs) from MODIS and global
693 biodiversity. Remote Sensing of Environment 222, 204–214. <https://doi.org/10.1016/j.rse.2018.12.009>
- 694 Radeloff, V.C., Roy, D.P., Wulder, M.A., Anderson, M., Cook, B., Crawford, C.J.,
695 Friedl, M., Gao, F., Gorelick, N., Hansen, M., Healey, S., Hostert, P., Hulley,
696 G., Huntington, J.L., Johnson, D.M., Neigh, C., Lyapustin, A., Lymburner, L.,
697 Pahlevan, N., Pekel, J.-F., Scambos, T.A., Schaaf, C., Strobl, P., Woodcock,
698 C.E., Zhang, H.K., Zhu, Z., 2024. Need and vision for global medium-resolution
699 landsat and sentinel-2 data products. Remote Sensing of Environment 300,
700 113918. <https://doi.org/10.1016/j.rse.2023.113918>
- 701 Razenkova, E., Farwell, L.S., Elsen, P., Carroll, K.A., Pidgeon, A.M., Radeloff, V.,
702 2022. **Explaining bird richness with the dynamic habitat indices across the con-**
703 **terminous US** 2022, B15A–05.
- 704 Razenkova, E., Lewińska, K.E., Yin, H., Farwell, L.S., Pidgeon, A.M., Hostert, P.,
705 Coops, N.C., Radeloff, V.C., n.d. Medium-resolution dynamic habitat indices
706 from landsat satellite imagery. Remote Sensing of Environment.
- 707 Roman, L.A., Pearsall, H., Eisenman, T.S., Conway, T.M., Fahey, R.T., Landry,
708 S., Vogt, J., Doorn, N.S. van, Grove, J.M., Locke, D.H., Bardekjian, A.C., Bat-
709 tles, J.J., Cadenasso, M.L., Bosch, C.C.K. van den, Avolio, M., Berland, A.,
710 Jenerette, G.D., Mincey, S.K., Pataki, D.E., Staudhammer, C., 2018. Human
711 and biophysical legacies shape contemporary urban forests: A literature synthe-
712 sis. Urban Forestry & Urban Greening 31, 157–168. <https://doi.org/10.1016/j.ufug.2018.03.004>
- 713 Schweiger, A.K., Cavender-Bares, J., Townsend, P.A., Hobbie, S.E., Madritch, M.D.,
714 Wang, R., Tilman, D., Gamon, J.A., 2018. Plant spectral diversity integrates
715 functional and phylogenetic components of biodiversity and predicts ecosystem
716 function. Nature Ecology & Evolution 2, 976–982. <https://doi.org/10.1038/s41559-018-0551-1>
- 717 Skidmore, A.K., Coops, N.C., Neinavaz, E., Ali, A., Schaepman, M.E., Paganini,
718 M., Kissling, W.D., Vihervaara, P., Darvishzadeh, R., Feilhauer, H., Fernan-
719 dez, M., Fernández, N., Gorelick, N., Geijzendorffer, I., Heiden, U., Heurich,
720 M., Hoborn, D., Holzwarth, S., Muller-Karger, F.E., Van De Kerchove, R.,
721 Lausch, A., Leitão, P.J., Lock, M.C., Mücher, C.A., O'Connor, B., Rocchini,
722 D., Turner, W., Vis, J.K., Wang, T., Wegmann, M., Wingate, V., 2021. Priority
723 list of biodiversity metrics to observe from space. Nature Ecology & Evolution.
<https://doi.org/10.1038/s41559-021-01451-x>
- 724 Suttidate, N., Steinmetz, R., Lynam, A.J., Sukmasuang, R., Ngoprasert, D., Chutipong,
725 W., Bateman, B.L., Jenks, K.E., Baker-Whatton, M., Kitamura, S., Ziolkowska,
726 E., Radeloff, V.C., 2021. Habitat connectivity for endangered indochinese tigers

- 735 in thailand. *GLOBAL ECOLOGY AND CONSERVATION* 29. <https://doi.org/10.1016/j.gecco.2021.e01718>
- 736 Tachikawa, T., Kaku, M., Iwasaki, A., Gesch, D.B., Oimoen, M.J., Zhang, Z.,
737 Danielson, J.J., Krieger, T., Curtis, B., Haase, J., Abrams, M., Carabajal, C.,
738 2011. *ASTER global digital elevation model version 2 - summary of validation*
739 *results.*
- 740 Thomas, C.D., Cameron, A., Green, R.E., Bakkenes, M., Beaumont, L.J., Colling-
741 ham, Y.C., Erasmus, B.F.N., Siqueira, M.F. de, Grainger, A., Hannah, L.,
742 Hughes, L., Huntley, B., Jaarsveld, A.S. van, Midgley, G.F., Miles, L., Ortega-
743 Huerta, M.A., Peterson, A.T., Phillips, O.L., Williams, S.E., 2004. Extinction
744 risk from climate change. *Nature* 427, 5.
- 745 Thompson, I.D., Mackey, B., McNulty, S., Mosseler, A., 2009. Forest resilience,
746 biodiversity, and climate change: a synthesis of the biodiversity / resiliende /
747 stability relationship in forest ecosystems, CBD technical series. Secretariat of
748 the Convention on Biological Diversity, Montreal.
- 749 Urban, M.C., 2015. Accelerating extinction risk from climate change. *Science* 348,
750 571–573. <https://doi.org/10.1126/science.aaa4984>
- 751 Walter, J.A., Stovall, A.E.L., Atkins, J.W., 2021. Vegetation structural complex-
752 ity and biodiversity in the Great Smoky Mountains. *Ecosphere* 12, e03390.
753 <https://doi.org/10.1002/ecs2.3390>
- 754 Waring, R.H., Coops, N.C., Fan, W., Nightingale, J.M., 2006. MODIS enhanced
755 vegetation index predicts tree species richness across forested ecoregions in the
756 contiguous U.S.A. *Remote Sensing of Environment* 103, 218–226. <https://doi.org/10.1016/j.rse.2006.05.007>
- 757 White, Joanne.C., Wulder, M.A., Hobart, G.W., Luther, J.E., Hermosilla, T., Grif-
758 fiths, P., Coops, N.C., Hall, R.J., Hostert, P., Dyk, A., Guindon, L., 2014. Pixel-
759 based image compositing for large-area dense time series applications and science.
760 *Canadian Journal of Remote Sensing* 40, 192212. <https://doi.org/10.1080/07038992.2014.945827>
- 761 Zhu, Z., Woodcock, C.E., 2012. Object-based cloud and cloud shadow detection
762 in Landsat imagery. *Remote Sensing of Environment* 118, 83–94. <https://doi.org/10.1016/j.rse.2011.10.028>
- 763
- 764
- 765
- 766